Applied Radiation and Isotopes 153 (2019) 108831

Contents lists available at ScienceDirect

Applied Radiation and Isotopes

journal homepage: www.elsevier.com/locate/apradiso

# Underground gamma-ray measurements of radium isotopes from hydrothermal plumes in the deep Pacific Ocean

Mikael Hult[a,*], Matthew Charette[b], Guillaume Lutter[a], Gerd Marissens[a], Paul Henderson[b], Katarzyna Sobiech-Matura[a], Hardy Simgen[c]

[a] EC JRC, Retieseweg 111, B-2440, Geel, Belgium
[b] WHOI, Woods Hole, MA, 02543, USA
[c] Max-Planck-Institut für Kernphysik, Saupfercheckweg 1, D-69117, Heidelberg, Germany

## HIGHLIGHTS

- Metrology of detecting $^{226}$Ra and $^{228}$Ra in samples from hydrothermal plumes.
- Optimisation of parameters to detect low-levels of $^{228}$Ra using γ-ray spectrometry.
- Detection limits of 1.5 mBq was achieved using 1-week measurement underground.
- Radon emanation was only 0.5%.
- Radiopurity of all materials involved were investigated.

## ARTICLE INFO

*Keywords:*
γ-ray spectrometry
HPGe detectors
Hydrothermal plume
Climate change
Underground laboratory
GEOTRACES

## ABSTRACT

The radium isotopes $^{226}$Ra and $^{228}$Ra can provide important data on the dynamics of deep-sea hydrothermal plumes that travel the oceans for decades and have great impact on the ocean chemistry. This study focuses on parameters important for obtaining low detection limits for $^{228}$Ra using gamma-ray spectrometry. It is present at mBq-levels in samples collected during the US GEOTRACES 2013 cruise to the Southeast Pacific Ocean.

## 1. Introduction

Radionuclides can serve as important tracers in oceanographic studies. Radium isotopes are naturally produced in ocean sediments and rocks from alpha-decay of thorium isotopes. In a new science application the ratio of $^{228}$Ra ($T_{½}$ = 5.75 y) and $^{226}$Ra ($T_{½}$ = 1600 y) was measured to enable dating of oceanic waters impacted by the mineral rich hydrothermal vent discharges in the deep ocean (Kipp et al., 2018; Sanial et al., 2018; Van der Loeff et al., 2018). Iron (Fe) is an important micro-nutrient in the ocean and is present in relatively high concentrations in fluids emanating from hydrothermal vents. It is essential for photosynthesizing organisms in the marine environment and therefore indirectly affects the oceans' capacity to absorb $CO_2$. Work on better understanding ocean chemistry is much impacted by studying hydrothermal plumes (Tagliabue et al., 2010) and can ultimately result in better models for the ocean's role in regulating Earth's climate. As radium is emitted together with iron from vents (or black smokers as they are also called) and travel together in the naturally buoyant hydrothermal plumes, the radium-dating capacity can be used for understanding the dynamics and fate of iron in the plumes. The plumes can travel thousands of kilometres, including towards the ocean surface via mixing, and can therefore affect the marine life in entire oceans (Pavia et al., 2019).

In this study, samples from hydrothermal plumes collected during the 2013 US GEOTRACES expedition TN303, EPZT, GP16 (http://geotraces.org) to the East Pacific Rise were analysed using gamma-ray spectrometry. The measurements were performed using three different detector systems in the 225 m deep underground laboratory HADES. This article describes a number of metrological tests that were conducted to seek the optimal geometry and sample containers with respect to both detection efficiency and radiopurity. A specific challenge with these samples is that $^{226}$Ra is present at much higher activities

* Corresponding author.
*E-mail address:* mikael.hult@ec.europa.eu (M. Hult).

https://doi.org/10.1016/j.apradiso.2019.108831
Received 6 May 2019; Received in revised form 21 June 2019; Accepted 30 July 2019
Available online 31 July 2019

than $^{228}$Ra, between a factor 100 and 1000, and therefore swamps the gamma-ray spectrum and makes it difficult to detect $^{228}$Ra using its daughter $^{228}$Ac (Henderson et al., 2013). Therefore attempts to improve the $^{228}$Ra detection limits by enabling the $^{222}$Rn-daughters to escape the sample volume were also conducted in this study. A fact that facilitates the interpretation of $^{228}$Ra-results is that it is essentially unsupported by $^{232}$Th. Thorium–isotopes are exposed to many so-called scavenging reactions in ocean waters and are drastically depleted.

## 2. Materials and methods

### 2.1. Sampling and sample preparation

The samples in this study have been collected in the East Pacific Ocean down to 5000 m under the auspices of the international GEOTRACES programme (www.geotraces.org). The research vessel R/V *Thomas G. Thompson* sailed in October–December 2013 along a zonal cruise track from Peru to Tahiti and followed one plume from the Southern East Pacific Rise (SEPR) that was spreading in a westward direction (Moffett and German, 2018). Samples were collected every 80–500 km, with the closer station spacing occurring at the SEPR. The initial sample preparation and pre-concentration steps involved: 1) Pumping (up to 1600 L) of sea water using a McLane pump through a cartridge with $MnO_2$-coated acrylic fibres to absorb radium (Fig. 1). 2) Ashing of cartridges at 820 °C for 16 h 3) Transfer of ash (essentially $MnO_2$) to polystyrene measurement vials (Fig. 2). The amount of Mn-cartridge ash (from now referred to as $MnO_2$) produced varied; smaller ash weights were placed in 15 mm outer diameter polystyrene vials, while larger samples were added to 25 mm diameter vials. The vials were sealed using a two-part epoxy (West System 206 slow hardener + West System 105 epoxy resin) to prevent radon loss, thereby keeping $^{226}$Ra daughter products in equilibrium after a 4-week holding period (Henderson et al., 2013). To optimise detection of $^{228}$Ra, some samples (mainly from the large vials) were later transferred to PTFE (PolyTetraFluorEten) containers as shown in Fig. 2 as they have better geometry for measurement on coaxial HPGe-detectors compared to the vials.

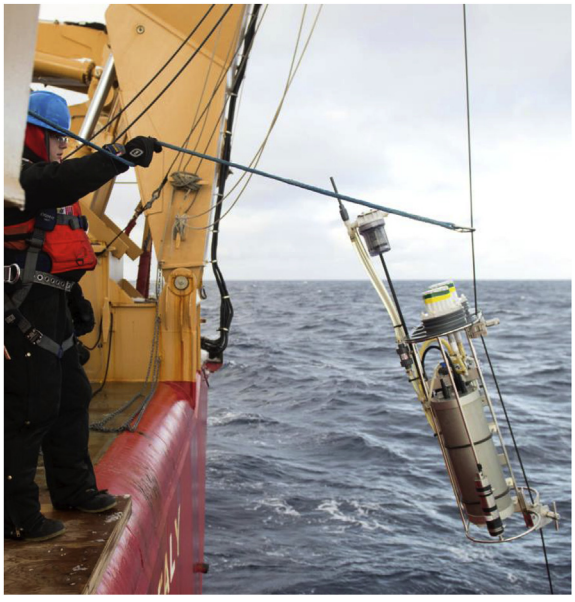

**Fig. 1.** Photo from the GEOTRACERS cruise GP16 with the McLane pump and the $MnO_2$-coated cartridge being deployed. Photo by Cory Mendenhall, U.S. Coast Guard.

**Fig. 2.** Photo of the two types of vials (left) and the PTFE container (right) used in this study.

### 2.2. Gamma-ray measurements

The gamma-ray spectrometry measurements of 37 samples were conducted in the period November 2017–October 2018. In addition, a metrological study using selected samples and reference samples were carried out. The first measurements were performed above ground, only to conclude that the obtained decision threshold of 20 mBq for $^{228}$Ac (in a sample with 4 Bq $^{226}$Ra measured on a low-background detector with a planar crystal of 80 mm diameter, 30 mm thick with point contact anode) was not sufficient. Therefore, the subsequent measurements were performed in the laboratory HADES (Andreotti et al., 2011), which is located 225 m underground at the premises of the Belgian nuclear centre SCK•CEN and is operated by EURIDICE (www.euridice.be). Three detector systems (with in total four HPGe-detectors (Ge4, sandwich and Ge14) were used for the measurements of quantifying $^{226}$Ra and $^{228}$ Ra in the samples. Table 1 gives an overview of their characteristics. However, in order to study the optimal geometry and measurement conditions, some samples were also measured on two additional detectors (Ge3 and Ge12) as indicated in Table 1. All detectors are specially designed ultra low-background detectors.

### 2.3. Radon emanation measurements

The $^{222}$Rn emanation measurement was carried out at MPI-K in Heidelberg using a high sensitivity system (Zuzel and Simgen, 2009). It was developed to test materials for experiments looking for rare events like Borexino and XENON1T. The ashed $MnO_2$ sample was placed in a small container (volume: ~5 cm$^3$) and connected to a much larger emanation vessel (volume: ~1000 cm$^3$) with a separation valve in between. Initially, both volumes were pumped to remove any residual radon. Then, the volumes were filled with 1 atm of $^{222}$Rn-free helium. During the subsequent emanation time (at least 10 days), the separation valve was open and emanating radon was allowed to distribute in the two volumes. Finally, the separation valve was closed and only the fraction of the $^{222}$Rn in the larger emanation vessel was measured in the following way: It was extracted from the helium carrier gas, purified and moved to an ultra low-level proportional counter (Wink et al., 1993), where its alpha decays were counted for a few hours. All operations were done at room temperature. The measurement was carried out three times and the final emanation rate of the ashed $MnO_2$ sample was obtained by averaging over the three individual results, which agreed within the measurement uncertainty (see Chapter 3.2).

### 2.4. Radon removal and radiopurity

Seeing that the samples contained almost a factor 1000 higher activity of $^{226}$Ra than of $^{228}$Ra it was not a challenge to measure $^{226}$Ra given that the $^{222}$Rn and its daughters were in secular equilibrium with

**Table 1**
Characteristics of the ultra low-background detectors used in this study.

| | Ge-3 | Ge-4 | Sandwich (dual detector system) | | Ge-12 | Ge-14 |
|---|---|---|---|---|---|---|
| | | | Ge-7 | Ge-15 | | |
| Rough description | "Standard" coaxial | Coaxial with a thin top deadlayer | Coaxial with a thin top deadlayer | Coaxial with a thin top deadlayer | "Standard" Well-detector | Well-detector with point contact anode and a thin inner deadlayer |
| Nominal top deadlayer thickness | 0.5 mm | 0.3 μm | 0.3 μm | 0.3 μm | 1 μm inside well | 50 μm inside well |
| Nominal side deadlayer thickness | 0.5 mm | 0.5 mm | 0.7 mm | 0.5 mm | 0.6 mm | 0.5 mm |
| Relative efficiency | 60% | 106% | 90% | 89% | n.a. | n.a. |
| FWHM at 338 keV | 1.76 keV | 1.70 keV | 1.58 keV | 1.11 keV | 1.79 keV | 1.05 keV |
| FWHM at 911 keV | 2.04 keV | 1.97 keV | 1.96 keV | 1.47 keV | 2.09 keV | 1.62 keV |
| FWHM at 1332 keV | 2.20 keV | 2.11 keV | 2.10 keV | 1.66 keV | 2.26 keV | 1.93 keV |
| Age (Jan. 2019) | 22 years | 19 years | 13 years | 2 years | 6 years | 3 years |
| Other characteristics | | | Inverted (looking down) | | Has a small planar crystal in the same cryostat | Point-contact anode |
| Reference | Hult et al., 2000 | Hult et al., 2003 | Wieslander et al. (2009) (Ge-15 replaced Ge-6 recently) | | n.a. | Hult et al. (2018) |

$^{226}$Ra and homogeneously distributed in the sample volume. However, detecting $^{228}$Ra proved more difficult as the major gamma-lines following the $^{228}$Ra decay, those at 338 keV, 911 keV and 969 keV following the decay of its daughter $^{228}$Ac (which is in secular equilibrium with $^{228}$Ra) sit on the Compton continuum generated by gamma-lines from the $^{222}$Rn-daughters. A number of tests were made to try to remove the $^{222}$Rn from the sample with the aim of improving the detection limits for $^{228}$Ra. These tests are described in Section 3.2.

Seeing that the radon-emanation is not high, an investigation was made to increase the emanation by heating the $MnO_2$ ash to 80 °C and 100 °C for 24 h and then starting a new measurement and collecting a spectrum every second hour.

With the aim to check the homogeneous distribution of radon-daughters, a study was also carried out to investigate the amount of radon-daughters that were implanted in the polystyrene-vial following the recoil of the decay of $^{222}$Rn. This was done by rapidly sawing off the vial at the height of where the epoxy plug is sitting and then emptying the vial of $MnO_2$. A quick rinse with deionised water was performed so that no residue could be seen in the vial. Four minutes after emptying the vial a measurement was started and a spectrum recorded every 10 min.

Finally, a number of measurements were carried out in HADES to study the radiopurity of materials involved in the study. First, the empty polystyrene vials were measured. Then, two samples of "unexposed" (i.e., not used for filtering sea water), ashed $MnO_2$-powder were measured. Except for the exposure to sea water, they had been treated in an identical manner to the actual samples. The powder/ash was thus also contained in a polystyrene vial that was sealed with epoxy. The last radiopurity measurements concerned 245 g of a batch of the sealing epoxy used in the plug. It was also measured in HADES.

## 3. Results

### 3.1. Radiopurity

The results of the radiopurity measurements performed using gamma-ray spectrometry in HADES are summarised in Table 2. The activities of the empty vial and the epoxy seal are clearly really low and can be completely neglected for this application. There was no detection of radium in the blank samples. However, there is some activity of $^{4}$K, likely a residual of the $KMnO_4$ reagent used to prepare the cartridges. Due to the presence of several Bq of $^{226}$Ra in the actual samples, it is not a severe limitation that $^{4}$K is present at this level. However, future work on improving the sampling process may need to take this $^{4}$K activity into consideration.

**Table 2**
Results of radiopurity measurements using gamma-ray spectrometry in HADES of materials involved in the study. Reference date: 1 January 2019. Decision thresholds are calculated according to the ISO11929:2010 standard with $\alpha = 0.05$.

| Radionuclide | Empty vial | Epoxy for seal | | Blank[a] ashed $MnO_2$ | |
|---|---|---|---|---|---|
| | mBq | mBq/kg | μBq[b] | mBq/g | mBq[b] |
| $^{228}$Ra | < 1.5 | < 18 | < 15 | < 1.6 | < 17 |
| $^{228}$Th | < 0.8 | < 13 | < 10 | < 0.41 | < 4.2 |
| $^{238}$U | < 3.5 | < 79 | < 7 | < 3.8 | < 39 |
| $^{226}$Ra | < 0.8 | < 12 | < 10 | < 0.41 | < 4.2 |
| $^{210}$Pb | < 7.0 | < 2000 | < 1700 | < 16 | < 160 |
| $^{4}$K | < 16 | < 72 | < 60 | 540 ± 55 | 5400 ± 550 |
| $^{137}$Cs | < 0.5 | < 6 | < 5 | < 0.29 | < 2.9 |

[a] Never used for adsorbing radium in sea-water.
[b] Activity in one typical sample.

### 3.2. Removal of $^{222}$Rn and activity in vial-walls

As a first test, a vial was cut just below the epoxy seal/plug (so that the top of the sample was exposed to air) and a measurement repeated on the same detector. This resulted in a surprisingly minute (non-significant) change of count rate at 609 keV, indicating that $^{222}$Rn is trapped in the $MnO_2$ sample. As a next step, the same sample was transferred to a Petri dish that was placed on the same detector without any lid. This exposed a greater surface of the $MnO_2$ ash to air. In addition, it was expected that the flushing of boil-off liquid nitrogen that was led into the lead-shield would increase the removal rate of $^{222}$Rn from the sample. However, this measurement led only to a reduction of the count-rate of the 609 keV peak of 10%. It was clear that the radon emanation rate was quite low, which triggered a measurement of this entity as described in Section 2.3. The radon-emanation averaged over three measurements was 20.0 ± 1.1 mBq in a 9.21 g sample with a$^{226}$Ra activity of 4.1 Bq. Thus, the radon-emanation amounted to 0.5%. This value is low compared to materials like dry soil (20%), sand (7%), slag (1.6%) but similar to e.g. ceramic tiles (0.6%) (Bossew, 2003).

To enhance the possibilities of improving detection limits for $^{228}$Ac, tests were conducted in which the ashed $MnO_2$ was heated for 24 h as described in Section 2.4. The tests performed at 80 °C and 100 °C gave more or less the same result: The count-rate of the 609 keV peak after heat-treatment was reduced by a factor 2.7. The same count-rate as before the heat-treatment was obtained again after a few days when secular equilibrium was regained between $^{226}$Ra and $^{222}$Rn (Fig. 3).

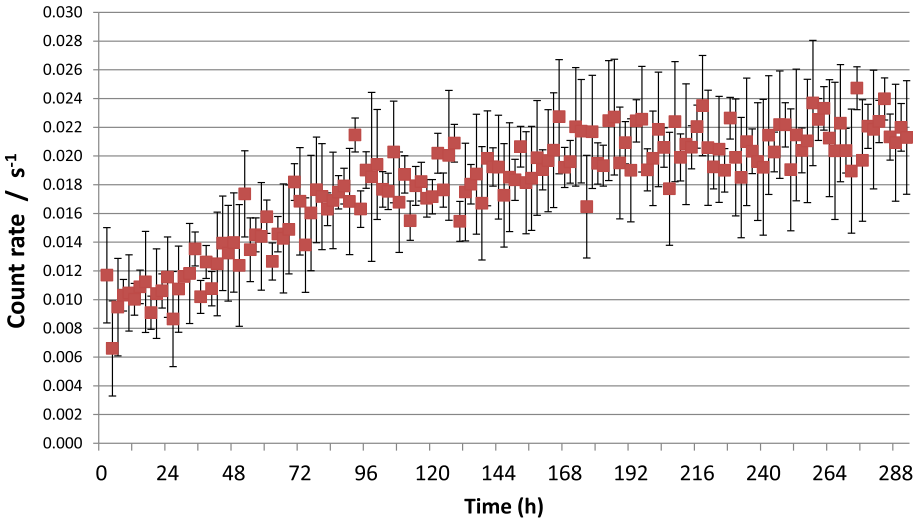


**Fig. 3.** The count-rate of the 609 keV peak as a function of the time after stopping a 24 h heating at 100 °C.

The measurement of the $^{214}$Pb and $^{214}$Bi "implanted" in the walls of the vial (as described in Section 2.4) had naturally poor counting statistics. But, by using the gross count-rate (instead of individual peaks) in each spectrum collected for 10 min it was possible to produce a decay curve with an approximate half-life of about 20 min, which was a strong indication of detection of radon-daughters from the walls of the vial. By extrapolating this decay-curve to zero (the time of emptying the vial) after subtracting the background count-rate of 513 counts per day (cpd), a count-rate of 1600 cpd was obtained. Seeing that the count-rate of a typical sample (on the same detector) was reaching 100,000 cpd, we can conclude that for the accuracy requested for this study, the effect of radon-daughters trapped in the vial-walls can be neglected.

### 3.3. Comparison of detectors

The spectrum obtained for each detector when measuring a typical sample (8 g ashed $MnO_2$ in a vial with 13 mm inner diameter) for one week is shown in Figs. 4 and 5 for the two energy intervals of interest for detecting $^{228}$Ra via $^{228}$Ac. For the coaxial detector systems (Ge3, Ge4 and sandwich) the vial was lying down on the endcap, centered by a specially made Perspex holder. The three peaks of interest (338 keV, 911 keV and 969 keV) are clearly visible. The $^{228}$Ac peak at 965 keV cannot be used due to interference from a gamma-ray at 964 keV following the decay of $^{214}$Bi. It is obvious from the figures that for Ge3 the peaks are below decision threshold. Calculations show that for the other four detector systems, all three peaks are above decision threshold. It is clear from the figures that Ge14 has the best signal-to-continuum ratio, which is further described by numbers in Table 3.

From a metrological point of view it is a better geometry for a coaxial HPGe-detector if the sample is disk-shaped. Therefore a number of samples were transferred to PTFE-containers as shown in Fig. 2. There was, however, only a very slight improved detection efficiency compared to having the original vial lying down.

### 3.4. Oceanographic results

Details of the oceanographic impact will be discussed in detail in dedicated articles in oceanographic journals. A brief analysis of the results shows that the activities of both $^{226}$Ra and $^{228}$Ra are consistent with the expected oceanographic distribution of these radionuclides

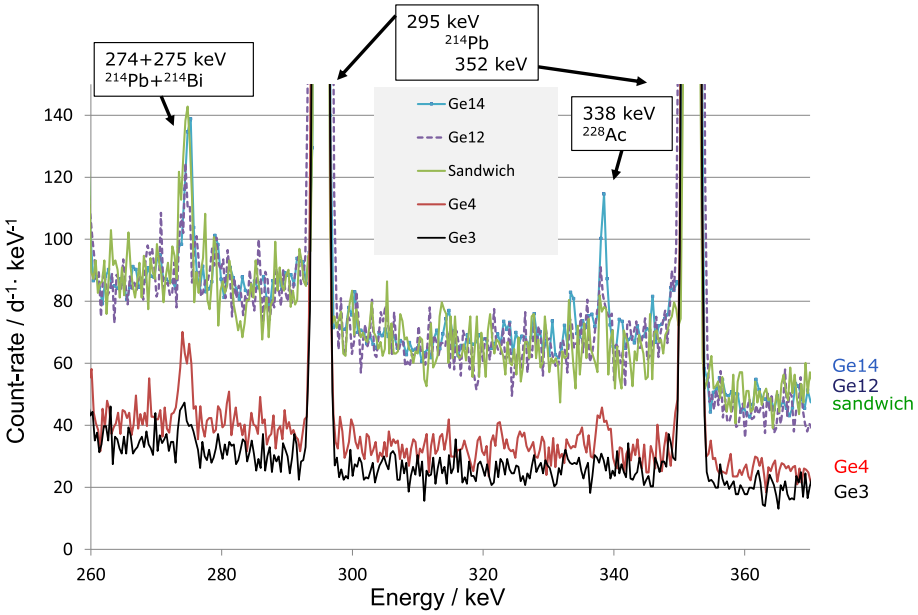


**Fig. 4.** Spectra from five detectors measuring the same ashed $MnO_2$ sample.

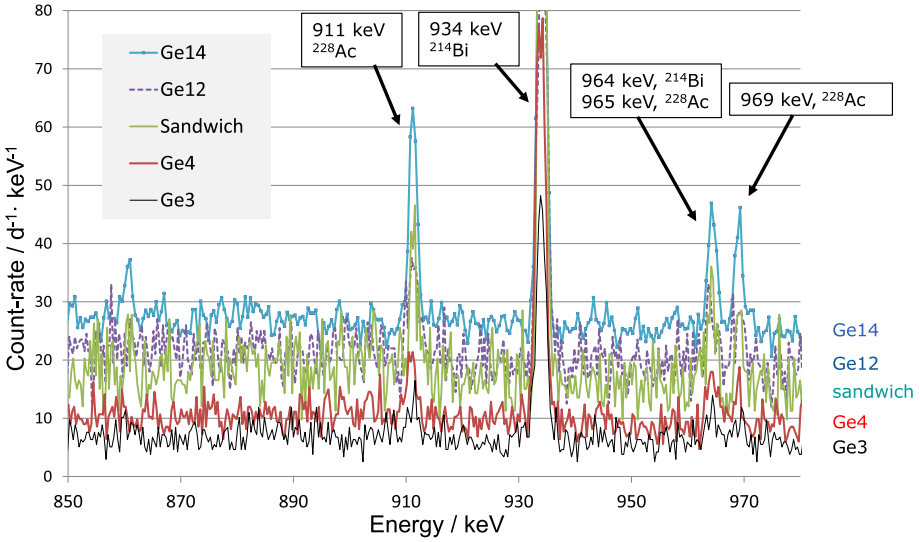


**Fig. 5.** Like Fig. 4 but for the energy interval 850–980 keV.

(Pavia et al., 2019). They show an increase in activity inside the hydrothermal plume compared to the surrounding water mass. For samples in the water column above the hydrothermal plume, they show a general decrease with depth, consistent with the known distribution of $^{228}$Ra in the surface ocean (Sanial et al., 2018). Furthermore, the age of the plume can be deduced from the decrease in $^{228}$Ra-activity as a function of the distance from the hydrothermal vent.

## 4. Discussion and conclusions

Generally speaking, the oceans are vastly unexplored. Considering their great impact on the Earth's climate and biodiversity one can argue that more scientific studies are needed. In recent years the field of underground gamma-ray spectrometry has grown considerably and can enable oceanographers with important tools to perform more advanced and diversified studies. For the samples in this study the detection of $^{228}$Ra (via $^{228}$Ac) was particularly interesting as most of the samples had activities below detection for conventional above ground labs and near to the decision threshold of the underground detector systems. Therefore, also smaller improvements made a difference to this study as it enabled values to go from below to above decision threshold. Future improvements in measurement techniques can also positively impact oceanographic expeditions like GEOTRACES by enabling sampling of smaller water volumes (and thereby saving time) or by collecting samples from depths were the radium concentrations are lower (further away from vents and other sources).

When focussing on the gamma-ray spectrometry measurements, one important conclusion for successfully detecting low levels of $^{228}$Ra in this type of marine samples with relatively high levels of $^{226}$Ra is to start measurements shortly (within a year) after sampling to minimise the effect of the $^{228}$Ra decay. The measurements reported herein were carried out 4–5 years after the research cruise, which means that the $^{228}$Ra activity was only 61%–54% of the activity at the time of sample collection. However, seeing that the gamma-rays of some thoron-daughters have high emission probability (238.6 keV, 583 keV and 2614 keV) it is possible to use these peaks as long as the state of (non-) equilibrium between $^{228}$Th (half-life 1.91 y) and $^{228}$Ra is taken into account (Charette et al., 2015), which generally will require multiple measurements a year or so apart. Waiting for transient equilibrium is also a possibility. For that to happen it is an advantage if long time elapses between sample collection and measurement. After 6 years, 90% of that transient equilibrium is reached. In this paper we did not discuss optimising the detection efficiency for those three gamma-lines. In brief one can say that the 238.6 keV line (following the decay of $^{212}$Pb) is excellently suited for well-detectors as there is very little coincidence summing effect. The peak at 2614 keV (from the decay of $^{208}$Tl) is highly useful in underground laboratories were the background at that high energy is essentially negligible (at least for a “short” 1–2 week measurement), but in big well-detectors it will suffer some loss from coincidence summing with the 583 keV line. Instead of waiting 6 years (or so) one can, as stated above, perform three measurements with sufficient delay in between to seek to establish at what stage towards equilibrium the system is although this is again putting a strain on the measurement capacity in underground detector-systems.

Another key conclusion was that the optimal measurement condition for these samples was in vials measured in detector Ge14, which is a new so-called SAGe-well detector. It has a thin (micro-metre sized) inner deadlayer and a point contact anode, which renders it superior energy resolution compared to “traditional” well-detectors (Hult et al., 2018). It is the energy resolution that gives this detector an extra edge in this study since this also reduces the impact of adjacent large peaks from radon-daughters on the small peaks from $^{228}$Ac. It has also an

**Table 3**
Comparison of detection efficiency and decision threshold for the 5 different detector systems (without correction for coincidence summing).

| Detector (relative eff. crystal type) | Sample configuration | FEP efficiency | | Decision threshold[a]/mBq | |
|---|---|---|---|---|---|
| | | 338 keV | 911 keV | 338 keV | 911 keV |
| Ge-3 (60% coaxial) | Vial lying down | 6.7% | 2.7% | 14 | 22 |
| Ge-4 (106% coaxial) | Vial lying down | 11% | 3.9% | 8 | 6 |
| Sandwich (2 × 90% coaxial) | Vial lying down | 16% | 6.6% | 9 | 7 |
| Ge12 ″standard” well | Vial | 19% | 6.4% | 10 | 9 |
| Ge14 point contact well | Vial | 31% | 14% | 2.2 | 1.5 |

[a] For a typical sample with 4.1 Bq of $^{226}$Ra measured for 7 days with reference time at the start of the measurement and at $\alpha = 0.05$ following ISO-11929:2010.

excellent peak-to-Compton ratio. The only drawback is that for cascading gamma-rays the coincidence summing effect is great. The sandwich detector system (Wieslander et al., 2009) consists of two detectors and has thereby lower losses from coincidence summing.

With the operating conditions stated above it is possible to measure one sample per week (after filtering 1600 L of sea water) and obtain a detection limit (at the time of the measurement) of $^{228}$Ra of about 2 mBq assuming the $^{226}$Ra activity is 4 Bq. By introducing the repeated heating of the sample and measuring for 2 weeks one can reduce this limit by a factor 2. Furthermore, by measuring immediately after sample collection the detection limit (with reference date at the time of sampling) will go down another factor 2 compared to this study. In oceanographic terms this means reaching detection limits for $^{228}$Ra in the order of 0.002 dpm/100 L (which is the commonly used unit in oceanographic literature), when pumping 1600 L sea water through the cartridges with $MnO_2$-coated acrylic fibres.

Other key conclusions from this study are

- The radon emanation from the ashed $MnO_2$ powder was found to be very low (~0.5%).
- Given the low radon emanation rate, one can conclude that the $^{222}$Rn and daughters were homogenously distributed in the sample volume when the sample was sealed. In fact, it may be possible to reach sufficient quantitative accuracy by measuring the vials without the seal by applying a small correction factor for $^{222}$Rn loss.
- The tests performed by heating the ashed $MnO_2$ showed that it is possible to reduce the count-rate from radon-daughters a factor 2.7. This is not an impressive reduction but for a few specific samples where the $^{228}$Ra activity is near the detection limit it could be worthwhile.
- The materials used in the US GEOTRACES 2013 project had an adequate level of radiopurity. One can, however, not assume that all future batches of the same materials will be radiopure, so radiopurity tests will be necessary in future work as well and should be undertaken already at the planning stage if practically possible.
- The activity of radon-daughters in the vial-walls could be detected and were sufficiently low to be disregarded in the quantitative analysis.

## Acknowledgements

The work of the HADES-staff of Euridice at SCK•CEN is gratefully acknowledged. We are most grateful to Dr. Faidra Tzika for her work in the precursor to this project. Many thanks to Heiko Stroh for quality control and measurements in HADES. This research was supported in part by grants from the U.S. National Science Foundation, Ocean Sciences division (OCE-1232669 and OCE-1736277).

## References

Andreotti, E., et al., 2011. Status of underground radioactivity measurements in HADES. In: Proceedings of the 3rd International Conference on Current Problems in Nuclear Physics and Atomic Energy, Kyiv. Publishing Department of KINR, pp. 601–605.

Bossew, P., 2003. The radon emanation power of building materials, soils and rocks. Appl. Radiat. Isot. 59, 389–392.

Charette, M.A., Morris, P.J., Henderson, P.B., Moore, W.S., 2015. Radium isotope distributions during the US GEOTRACES North Atlantic cruises. Mar. Chem. 177, 184–195.

Henderson, P.B., Morris, P.J., Moore, W.S., Charette, M.A., 2013. Methodological advances for measuring low-level radium isotopes in seawater. J. Radioanal. Nucl. Chem. 296 (1), 357–362.

Hult, M., Martinez-Canet, M.-J., Köhler, M., Das Neves, J., Johnston, P.N., 2000. Recent developments in ultra low-level γ-ray spectrometry at IRMM. Appl. Radiat. Isot. 53, 225–229.

Hult, M., Gasparro, J., Johansson, L., Johnston, P.N., Vasselli, R., 2003. Ultra Sensitive Measurements Using HPGe-Detectors in the Underground Laboratory HADES, Env. Radiochem. Anal. II. Royal Society of Chemistry, Cambridge, UK, pp. 373–382.

Hult, M., Marissens, G., Stroh, H., Lutter, G., Tzika, F., Marković, N., 2018. Characterisation of an ultra low-background point contact HPGe well-detector for an underground laboratory. Appl. Radiat. Isot. 134, 446–449.

Kipp, L.E., Sanial, V., Henderson, P.B., van Beek, P., Reyss, J.-L., Hammond, D.E., Moore, W.S., Charette, M.A., 2018. Radium isotopes as tracers of hydrothermal inputs and neutrally buoyant plume dynamics in the deep ocean. Mar. Chem. 201, 51–65. https://doi.org/10.1016/j.marchem.2017.06.011.

Moffett, J.W., German, C.R., 2018. The US GEOTRACES eastern tropical Pacific transect (GP16). Mar. Chem. 201, 1–5.

Pavia, F.J., Anderson, R.F., Black, E.E., Kipp, L.E., Vivancos, S.M., Fleisher, M.Q., Charette, M.A., Sanial, V., Moore, W.S., Hult, M., Lu, Y., Cheng, H., Zhang, P., Edwards, R.L., 2019. Timescales of hydrothermal scavenging in the South Pacific Ocean from $^{234}$Th, $^{230}$Th, and $^{228}$Th. Earth Planet. Sci. Lett. 506, 146–156. http://doi.org/10.1016/j.epsl.2018.10.038.

Sanial, V., Kipp, L.E., Henderson, P.B., van Beek, P., Reyss, J.L., Hammond, D.E., Hawco, N.J., Saito, M.A., Resing, J.A., Sedwick, P., Moore, W.S., Charette, M.A., 2018. Radium-228 as a tracer of dissolved trace element inputs from the Peruvian continental margin. Mar. Chem. 201, 20–34. https://doi.org/10.1016/j.marchem.2017.05.008.

Tagliabue, A., Bopp, L., Dutay, J.-C., Bowie, A.R., Chever, F., Jean-Baptiste, P., Bucciarelli, E., Lannuzel, D., Remenyi, T., Sarthou, G., Aumont, O., Gehlen, M., Jeandel, C., 2010. Hydrothermal contribution to the oceanic dissolved iron inventory. Nat. Geosci. 3, 252–256. https://doi.org/10.1038/ngeo818.

Van der Loeff, M.R., Kipp, L., Charette, M.A., Moore, W.S., Black, E., Stimac, I., Charkin, A., Bauch, D., Valk, O., Karcher, M., Krumpen, T., Casacuberta, N., Smethie, W., Rember, R., 2018. Radium isotopes across the Arctic Ocean show time scales of water mass ventilation and increasing shelf inputs. J. Geophys. Res. Oceans 123, 4853–4873. https://doi.org/10.1029/2018JC013888.

Wieslander, J.S.E., Hult, M., Gasparro, J., Marissens, G., Misiaszek, M., Preusse, W., 2009. The Sandwich spectrometer for ultra low-level gamma-ray spectrometry. Appl. Radiat. Isot. 67, 731–735.

Wink, R., Anselmann, P., Dörflinger, D., Hampel, W., Heusser, G., Kirsten, T., Mögel, P., Pernicka, E., Plag, R., Schlosser, C., 1993. The miniaturized proportional counters HD-2(Fe)/(Si) for the GALLEX solar neutrino experiment. Nucl. Instrum. Methods A329, 541–550.

Zuzel, G., Simgen, H., 2009. High sensitivity radon emanation measurements. Appl. Radiat. Isot. 67, 889–893.